IUST Iran University of Science and Technology

Iranian Journal of Electrical and Electronic Engineering

Journal Homepage: ijeee.iust.ac.ir

Research Paper

Two-channel Power Supply for an Imaging System with Copper Bromide Vapor Brightness Amplifiers

E. Y. Burkin*, F. A. Gubarev**(C.A.), V. V. Sviridov*, D. V. Shiyanov***

Abstract: A two-channel pulsed power supply for an imaging system with brightness amplification and independent synchronous laser illumination is designed. The power supply generates synchronized high-voltage pulses with a frequency of 16–24 kHz, an average electrical power of up to 1.2 kW, and an adjustable amplitude of up to 6.2 kV to pump copper bromide gas discharge tubes with independent control of the temperature parameters of the active medium. To generate pumping pulses for laser media, we used a two-channel thyratron circuit with a common source of stabilized voltage provided by a step-down pulse stabilizer and a bridge inverter-based circuit for the pulsed charge of storage capacitors. The voltage equalization on the storage capacitors is carried out by means of magnetic coupling of the charging inductances wound on a common core. Adjustable delay lines based on variable inductances provide synchronous operation of two brightness amplifiers with a synchronization accuracy of lasing pulses of ±1 ns. The power supply demonstrated stable operation with two gas discharge tubes having different characteristics, including those with different types of electrodes. It has been integrated into a laboratory facility for the study of high-energy materials combustion.

Keywords: Pulsed Power Supply, High-Voltage Generator, Copper Bromide Laser, Master Oscillator-Power Amplifier System, High-Speed Imaging.

1 Introduction

ONE of the promising applications of a metal-vapor amplifying medium is its use in imaging systems for high-temperature processes and extreme states of matter-laser monitors [1-8].

Iranian Journal of Electrical and Electronic Engineering, 2023.
Paper first received 09 Aug 2022, revised 08 May 2023, and accepted 12 May 2023.
*The authors are with Laboratory of Pulse-Beam, Electric Discharge and Plasma Technologies, National Research Tomsk Polytechnic University, Tomsk, Tomsk Region, Russia.
E-mails: burkineyu@tpu.ru and vvsviridov@tpu.ru.
**The author is with Institute of Nuclear Energy and Industry, Sevastopol State University, Sevastopol, Crimea, Russia.
E-mail: gubarevfa@mail.ru.
***The author is with Laboratory of Quantum Electronics, V.E. Zuev Institute of Atmospheric Optics, Tomsk, Tomsk Region, Russia.
E-mail: shiyanov73@mail.ru.
Corresponding Author: F. A. Gubarev.
https://doi.org/10.22068/IJEEE.19.3.2617.

Laser monitors make it possible to solve the problem of imaging processes accompanied by intense background lighting and scattering of reaction products, in particular the problem of monitoring the surface of high-energy materials (HEMs) during combustion through the flame created by burning reagents [8].

The main approaches to laser monitoring are a monostatic scheme with one amplifying medium and a bistatic scheme with two laser media. The monostatic scheme has two main limitations: the imaging distance is limited by the duration of the quantum amplifier emission pulse [9]; the illuminance of the imaging area can only be increased by increasing the power of the amplifier. The bistatic scheme of the laser monitor is based on the principle of amplifying the radiation of the illumination laser by the second active medium,

similar to the amplification of power in the "master oscillator-power amplifier" system [10, 11]. Such a system is more complex; as a rule, it has two synchronized high-voltage pumping sources. Until recently, a bistatic laser monitor was considered for the visualization of distant objects under conditions of intense background lighting [6, 12]. In this case, the use of powerful laser systems with an illumination power of 8–10 W was assumed.

Flammable HEMs are a specific target of research using a laser monitor, in particular, the process of their initiation by laser radiation [13]. Laser illumination of the imaging system can affect the ongoing thermal processes and the surfaces of the reacting materials. Therefore, one of the key challenges in developing an imaging system for flammable HEMs is to minimize the impact of illumination in the laser monitoring area while maintaining high image quality. In [14, 15], we demonstrated the possibility of using a laser monitor with independent illumination to study the initiation and combustion of metal nanopowders, including the use of a gas discharge tube (GDT) with capacitive electrodes [15]. Independent illumination gives a significant increase in the brightness and sharpness of laser monitor images at a relatively low (a few milliwatts per mm^2) laser illumination power density.

Operating with GDTs with independent stabilization of temperature parameters, a low level of power consumption of each GDT makes it possible to build a common power source with the division of the output power into channels as close as possible to the output, in order to eliminate channel imbalance. This paper presents the results of the development and study of a two-channel pumping source based on a single source of pulsed charging of storage capacitors, in which the GDT operating point is equalized in the two-channel mode using a two-winding equalization inductor, which ensures charging of the storage capacitors of both GDTs.

The paper also discusses the design features and modes of operation of low-power amplifying media on copper bromide vapors with independent control of temperature parameters. Considerable attention is paid to minimizing the mass and overall parameters of the laser system to design a prototype of a laser monitor with an independent laser illumination.

2 Copper Bromide Gain Media with Independent Control of Temperature Parameters

In this work, the approach of independent heating of the active part and containers with copper bromide is used in the active elements. Unlike self-heating systems [10, 16-19] and systems with common heating of the active part and containers with copper bromide [20], independent heating allows the implementation of modes with a reduced energy input to the discharge, in which the temperature parameters of the active medium are practically independent of pumping power [21–25]. In [2], to monitor the combustion process, a laser monitor with a copper bromide vapor brightness amplifier with independent heating was used. The gain media of 5 cm in diameter and 90 cm long emits an average lasing power of 6–12 W with plane-parallel resonator and an average power of amplified spontaneous emission (ASE) 0.5–2 W at 1.5 kW average pumping power.

In fact, ASE is radiation that illuminates the observation surface, so the question of its effect on the object of study is obvious. When studying the coarse $FeTiO_3$+SiO_2+Si+Al+C and Ni+Al powders in [2], the ASE power was 0.5 W and did not affect the observed object. In contrast, when studying aluminum nanopowder in [8] at an average power of 65 mW, we could observe a visible change in the surface and even uncontrolled initiation when adjusting the optical scheme. We have experimentally found that the ignition threshold of nanoAl in a traditional laser monitor scheme is 250 mW/mm^2 with an exposure time of 2 ms. Insignificant visible changes on the surface begin at an ASE power of 130 mW/mm^2.

To ensure the operation of the brightness amplifier in the low pumping power mode and to minimize the size of the laser monitor, the following modification of the active element of the brightness amplifier was carried out. The refractory brick, fixed with a steel casing, is replaced by a kaolin heat-insulating plate, which simultaneously serves as a seat for a quartz GDT (Fig. 1). The active elements in the proposed configuration are separated from the pumping source and connected to it by coaxial cables. This made it possible to place the GDT with heaters and thermostats in a lightweight housing. The thermostats had an accuracy of temperature stabilization of ±1 ºC. In

the work, three brightness amplifiers (BA) of different active volumes were used (Table 1). BA1 and BA2 had traditional internal electrodes, and BA3 had external capacitive electrodes. The operation of capacitively pumped active elements is considered in more detail in [24, 25]. In this work, the electrodes had dimensions of 29 cm/6.5 cm (length/diameter); the calculated value of the electrodes capacitances *Ce1*=*Ce2*=524 pF, the GDT equivalent capacitance C_{cap}=262 pF. The consideration of capacitive GDT was of interest in this work from the point of view of the universality of the developed power supply.

In a GDT with independent stabilization of the temperatures of the active part and containers with copper bromide, the operation mode for the concentration of copper bromide vapors slightly depends on the energy input into the discharge from the high-voltage power supply. In this case, with lower pumping power, the effect of the discharge circuit inductance is smaller [22]. Moreover, the proportion of yellow radiation does not increase. It should also be noted that working without the addition of HBr has the advantage of a smaller effect of the discharge circuit inductance on the lasing energy. The HBr additive is often used to increase the lasing power of CuBr-laser and smooth the beam profile when the active element operates in the laser generation mode [16-21]. Taking into account the significant flattening of the gain profile during the propagation of beams carrying an image in a laser monitor [9], the use of HBr additive is inappropriate. Therefore, when developing the pumping source in this work, we assumed operation without the addition of HBr.

3 Synchronized Two-channel Source of High-voltage Pulses

Traditional pumping circuits for active metal vapor media are pulse-charging capacitance transfer circuits switched by thyratron [16, 17]. The pulse-repetition frequency of 20±5 kHz and the value of the storage capacitance of units nanofarads can be considered typical values for pumping circuits of the active medium on copper bromide vapors [20–23].

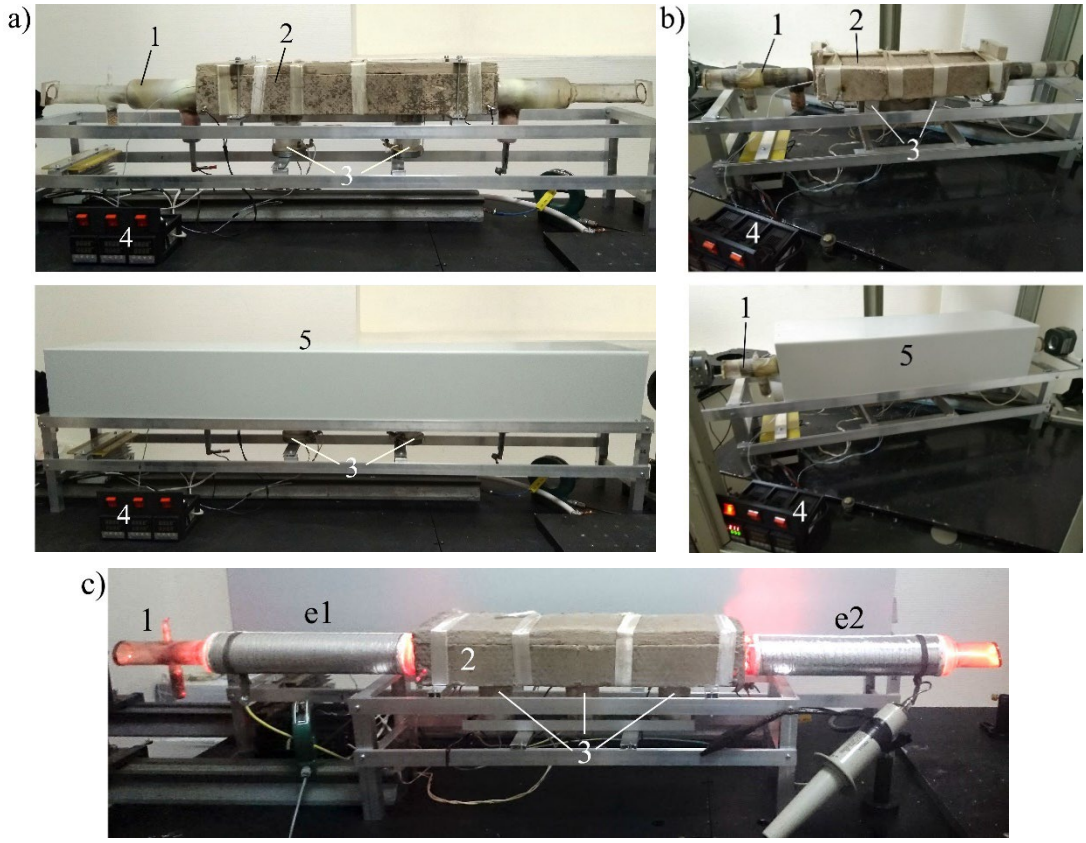

Fig. 1 Photographs of the active elements of the brightness amplifiers. (a) BA1; (b) BA2; (c) BA3; 1 – silica GDT; 2 – heater of the active part; 3 – heaters of the copper bromide containers; 4 – temperature controller; 5 – metal shield; e1, e2 – capacitive electrodes.

Table 1 Gas-discharge tubes parameters.

Name	Inner diameter, cm	Active length, cm	Electrode type	ASE, mW	Two-pass lasing, mW
BA1	3.0	60	Inner	22	410
BA2	1.5	50	Inner	14	270
BA3	2.0	50	Capacitive	25	245

At such operating frequencies, a single-pulse charge of the storage capacitance usually proceeds from a voltage source through a ballast inductor and a high-voltage diode [26–28]. The charging process in this case is resonant with a doubling of the voltage across the capacitance with respect to the input voltage. When one power supply is used for two GDTs with non-identical parameters such as diameter, length, gas composition, etc., the problem of energy balancing of the GDT operating point arises. This problem can be solved for a particular case by selecting a storage capacitance, and it does not provide long-term stability if the GDT characteristics change. In the proposed power supply, the equalization of the GDT operating point in the two-channel mode is carried out using an equalizing inductor, which provides charge for the storage capacitors of both GDTs.

3.1 Structural Scheme

Structurally, the power supply is located in two modules (Fig. 2). The block diagram of the power supply is depicted in Fig. 3. The input rectifier, voltage stabilizer, inverter, transformer-rectifier unit, and digital control unit are located in the inverter module. This module dimensions are 480×480×130 mm^3. The second module contains thyratrons, charge transfer circuits, equalizing inductor, thyratron heater transformers, and triggering circuit. The dimensions of the thyratron module are 400×200×360 mm^3. This two-module configuration allows the pumping system to be placed in a more compact manner since individual units take up little space and can be placed in the most convenient places of the laboratory setup.

Both modules are powered by a standard 230 V, 50 Hz network. The input main voltage is supplied to the rectifier and passive input filter through the input switching and protective equipment, as well as the input noise-suppression filter. A constant unstabilized voltage of about 300 V at the filter output supplies the voltage regulator, which provides stabilization and regulation of the voltage at the input of the bridge inverter. The inverter output is connected to the primary winding of the step-up transformer. The high voltage pulse from the secondary winding of the transformer through the rectifier is fed to a two-channel modulator located in the thyratron module. Pump pulses are transmitted from the thyratron module to the GDTs through identical coaxial cables.

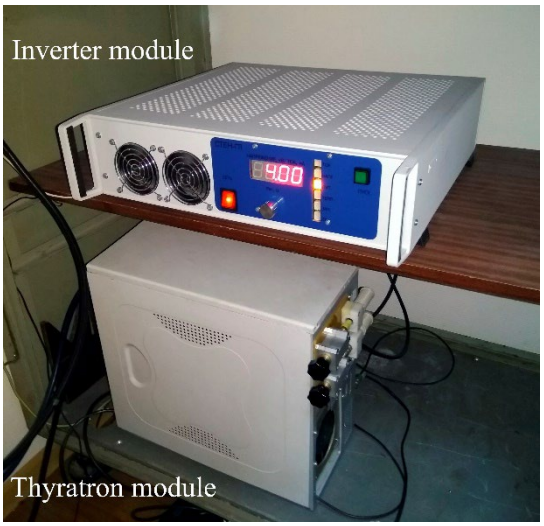

Fig. 2 Power supply.

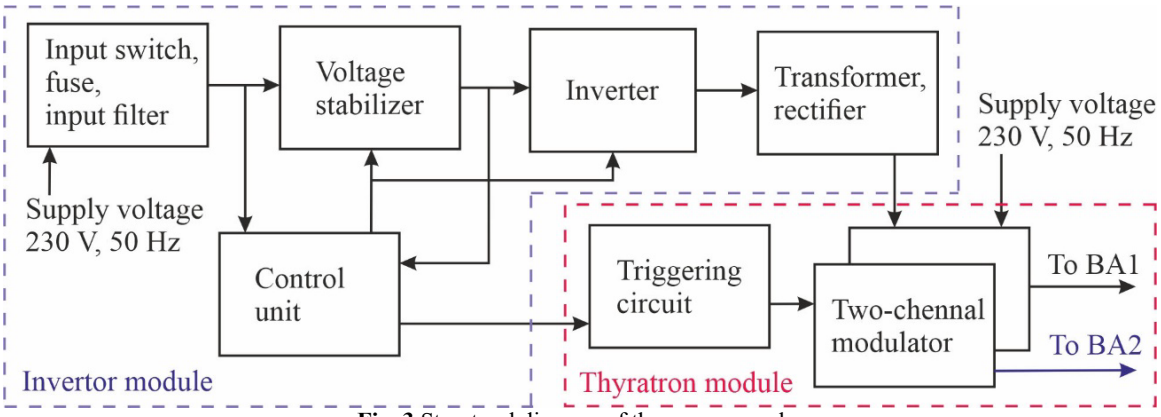

Fig. 3 Structural diagram of the power supply.

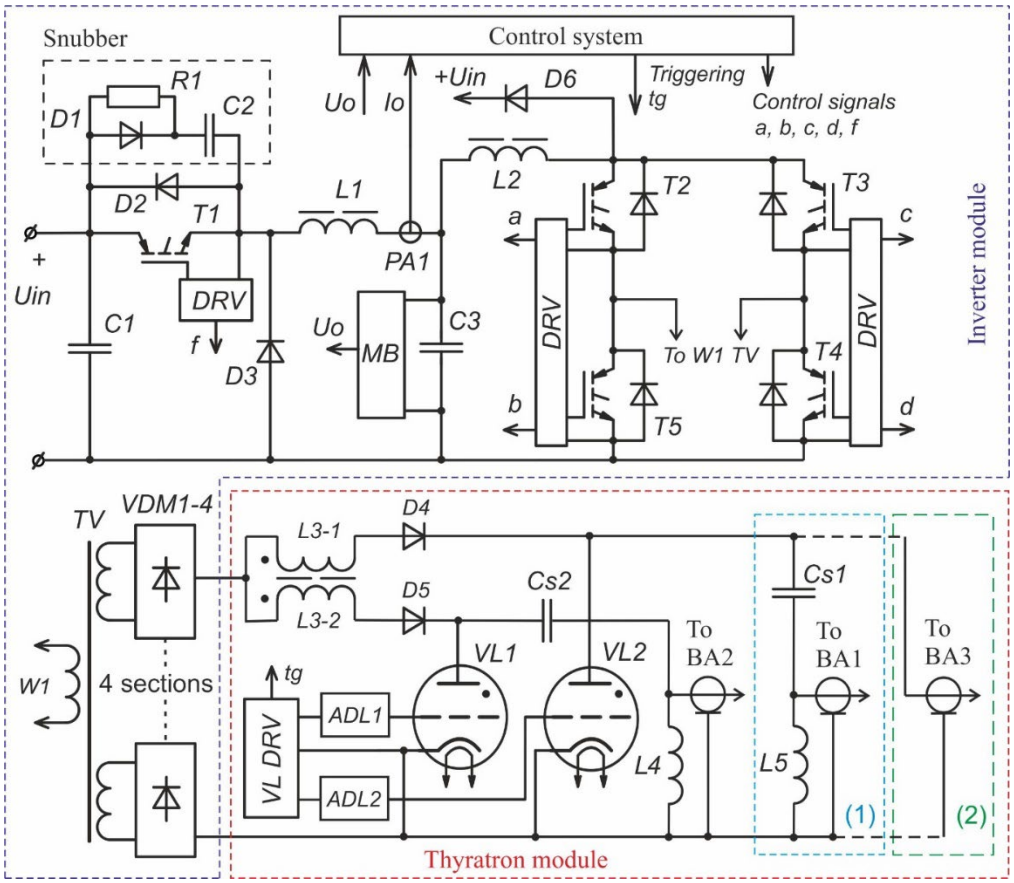

Fig. 4 Electrical circuit. (1) BA1 is connected, BA3 is disconnected; (2) BA3 (capacitive) is connected, BA1 is disconnected.

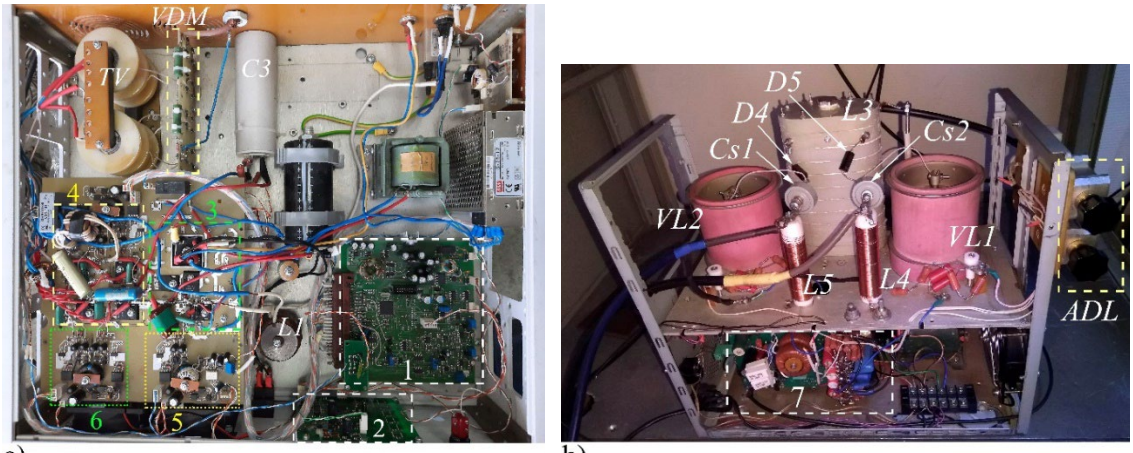

Fig. 5 Internal arrangement of elements in the modules: (a) – inverter module; (b) – thyratron module. 1 – control system board; 2 – indicator board; 3 – input downconverter; 4 – bridge inverter; 5 – voltage sensor *MB*; 6 – power transistor control driver; 7 – thyratron triggering drivers; *L1* – inductor of the input converter; *TV* – high-voltage transformer; *VDM* – output rectifier; *C3* – input capacitor of the inverter; *VL1*, *VL2* – thyratrons; *L3* – surge inductor; *Cs1*, *Cs2* – storage capacitors; *D4*, *D5* – diodes; *L4*, *L5* – by-pass inductors; *ADL* – adjustable delay lines.

3.2 Power Supply Circuitry

The fragments of electrical circuit of the power supply and the internal arrangement of elements in the modules are presented in Fig. 4 and Fig. 5, respectively. The basic parameters of the electrical circuit are given in Table 2. The input regulator from a single-phase AC network consists of a series-connected bridge rectifier with an input noise suppression filter, switching and protective circuits and an output smoothing LC-filter at the output of which an unstabilized DC voltage of 300 V is formed with a given ripple level.

Table 2 Electrical Circuit Basic Parameters.

Name	Type	Name	Type / Value	Name	Value
T1–T5	SPW47N60C3	*PA1*	CSNF161 (W1=4)	*L1*	2.08 mH
D3	C4D10120	*MB*	HCPL788J	*L3-1*	18 mH
D4, D5	UX-15B	*C3*	30 μF	*L3-2*	18 mH
D6	HFA16PB120	*Cs1*	1.0 nF	*L5*, *L4*	0.1 mH
DRV	TLP250	*Cs2*	0.68 nF	K_{TV}	12

An auxiliary filter capacitor precharge circuit is used to limit inrush currents at turn-on. The control system and other low-voltage auxiliary systems are powered by the mains auxiliary power supply. The voltage from the DC bus is fed to a switching voltage regulator.

The voltage stabilizer is designed as a step-down DC voltage converter. Its main elements are the power transistor *T1*, the reverse current diode *D3* and the output inductor *L1*. The ripple of the output voltage is smoothed out by capacitor *C3* (30 μF). Ripple factor did not exceed 3%. The switching frequency of the transistor *T1* is twice the frequency of the inverter transistors *T2–T5* and is equal to 40 kHz for the nominal mode of the output pulse frequency of 20 kHz. The snubber circuit serves for reducing dynamic losses in the transistor *T1* when it is turned off. When the frequency of the output pulses is varying, a proportional change in the switching frequency of transistor *T1* occurs. This mode ensures the identical formation of the output pulse voltage of the storage devices in each cycle of the inverter. The pulse drivers *DRV* by the signals *a-f* generated by the control system switch the transistors *T1–T5*. The regulation and stabilization of the voltage across the capacitor *C3* is carried out using feedback signals U_0 and I_0, the magnitude of which is proportional to the voltage U_{C3} and current I_{L1}, respectively. The feedback voltage is formed by the sensor (*MB*) based on the HCPL788J isolation amplifier chip. The *L1* inductor current feedback is formed using a current sensor CSNP161. In the control unit, a slave regulation principle is implemented, where the current I_{L1} is used as an internal variable and the voltage U_{C3} is used as an external variable.

The output voltage stabilizer link is a PI-controller with limited output voltage range and controller saturation. A link is implemented in digital form with an output to a digital-to-analog converter (DAC). The signal from the DAC output is fed to the analog link of the current regulator of the *L1* inductor as a master. The current regulator is an inertia-boosting link based on an operational amplifier. Diodes *D1* and *D2*, resistor *R1* and capacitor *C2* form a circuit to reduce dynamic losses in transistor *T1* and protect against overvoltage when turned off.

The digital control of the converter is implemented using the signal processor TMS320F2808. Feedback signals for the implementation of the control algorithm are the inductor current of the input current regulator and the output voltage of the voltage regulator. All signals come from the appropriate sensors, providing their isolation, filtering, and matching with the analog-to-digital converter of the processor. The control signals determine the synchronous operation of the pairs of transistors *T2–T4* and *T3–T5*. The duration of the active and passive phases is selected in such a way that the processes of charging the storage capacitors *Cs2*, *Cs1*/C_{cap} and the process of recuperation of the residual energy in the discharge circuit of these capacitors are completed. The storage capacitors *Cs2* and *Cs1* are charged through the inductance *L3-1* and *L3-2*, diodes *D4*, *D5* and by-pass inductances *L5*, *L4*, respectively. In the case of capacitive BA3 C_{cap} is charged through the plasma resistance.

The triggering circuit provides synchronization of the thyratrons *VL1*, *VL2* (TGI1-1000/25) and the charge of the storage capacitors. It consists of a single-channel transistor modulator (*VL DRV* with MOSFET STP21N90K5) and two adjustable delay lines *ADL1* and *ADL2*. Each adjustable delay line (ADL) contains a variable inductance, the value of which is changed by smoothly moving the ferromagnetic cores inside the inductors (ferrovariometers). We believe that the proposed triggering circuit can be used not only with TGI1-1000/25 thyratrons, but also with other commercially available analogs, including those with a non-heated cathode [29].

3.3 Data Recording

Measurement of the electrical characteristics was carried out using the voltage probes Tektronix P6015A and current sensor Pearson Current

Monitor 8450. Thorlabs DET10A/M high-speed photodiodes were installed to register laser radiation pulses. The output signals of the sensors were recorded with a Tektronix TDS-3054C oscilloscope. An Ophir Orion PD300 power meter was used to measure the average lasing power.

4 Power Supply Operation

The equivalent circuit of the charging process is shown in Fig. 6. Figure 7 presents the oscillograms of the voltage on the thyratron and the current of the primary winding of the transformer *TV* for two cases: 1) the charge of the capacitances *Cs1*=1000 pF, *Cs2*=680 pF and 2) *Cs2*=680 pF and C_{cap}=262 pF. The charging process starts when the control signal turns on the transistors on one of the diagonals of the inverter (*T2-T4* or *T3-T5*). The stabilized voltage of the capacitor *C3* is applied through the inductor *L2* to the primary winding of the transformer *TV*, this voltage, transforming into the secondary winding, causes an oscillatory process of charging the storage capacitors *Cs1* and *Cs2*. The presence of the transformer leakage inductance *Ls* and the output parasitic capacitance *Co* leads to high-frequency oscillations in the current of the primary winding. The presence of these oscillations has practically no effect on the significantly slower process of charging the capacitors *Cs2, Cs1*/C_{cap}.

The inductances *L2*, *Ls*, *L4*, *L5* are relatively small compared to the magnetically coupled inductances *L3-1, L3-1* and practically do not affect the "slow" processes caused by the circuit consisting of the inductances *L3-1, L3-1* and the storage capacitors *Cs1* and *Cs2*. Thus, a simplified equivalent circuit can be represented as an input DC voltage source, a magnetically coupled inductor, and output capacitors. Since *L3-1, L3-1* dominates, we also do not take into account the magnetizing inductance *Lm* in a qualitative analysis of the processes in the charge circuit. The presence of a magnetic connection between the inductor windings determines the equality of the voltages on the windings of *L3-1* and *L3-2*. The action of the magnetic coupling has an equalizing effect on the voltages of the capacitors during their charging. As long as the circuit current is flowing during the charging process, the voltage across the capacitors *Cs1*, *Cs2* changes according to the same law (almost synchronously). The presence of other components leads to some non-ideal voltage equalization across the capacitors; however, it remains.

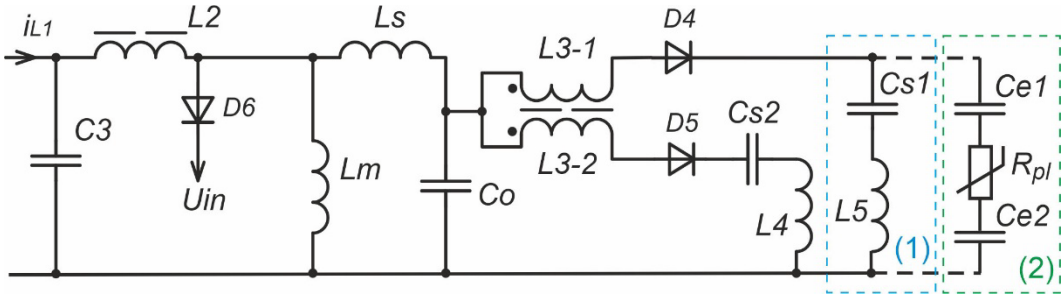

Fig. 6 Equivalent circuit of the process of charging storage capacitors *Cs2* and *Cs1*/C_{cap}. (1) – BA1 is connected, BA3 is disconnected; (2) – BA3 (capacitive) is connected, BA1 is disconnected.

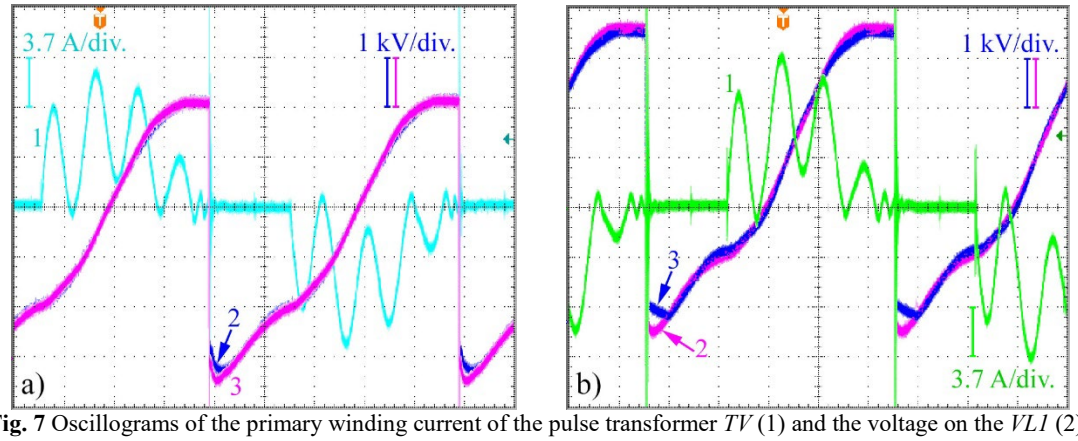

Fig. 7 Oscillograms of the primary winding current of the pulse transformer *TV* (1) and the voltage on the *VL1* (2) and *VL2* (3) anodes (approximately equal to the voltage on the storage capacitors). (a) – BA1 and BA2 connected, (b) – BA2 and BA3 connected.

At the end of the charge, the inverter transistors are turned off. The triggering circuit starts the thyratrons and the voltage pulses are applied to the GDT. In a laser monitor with independent illumination, the amplification is synchronized by controlling the switching times of two thyratrons in the excitation circuits, which are set by changing the arrival time of the trigger pulses on the thyratron grids. In the developed power source, the delay between the GDTs pumping pulses is varied by ADLs in the range from -50 to 50 ns with a synchronization accuracy of ±1 ns.

Figure 8 presents the oscillograms of the pumping and emission pulses for the different delays of ADLs. In these experiments, the illumination laser radiation is not fed into the brightness amplifier. Therefore, there is no mutual influence of the brightness amplifiers along the emission channel. In the first case (Fig. 8a), the pumping pulses of BA1 and BA2 arrive almost synchronously. The time shift between the emission pulses of ~10 ns is caused by the different nature of the breakdown due to the different geometry of GDTs. In the case in Fig. 7b, a delay of ~20 ns is introduced, which led to the corresponding mutual shift of the emission pulses of BA1 and BA2. Fig. 8c presents the oscillograms of the operation of a pair of active elements BA2 and BA3 with different types of electrodes.

The emission powers of the developed brightness amplifiers when working with the power supply presented in the work are given in Table 1. The maximum value of the power density at the object of study reached 60 mW/mm^2 in a short-focus laser monitor (F=8 cm). When using a 50 cm focus lens [13], the power density on the surface of the object did not exceed 0.85 mW/mm^2. The power density in the mirror-scheme laser monitor without illumination [9, 14] did not exceed 0.53 mW/mm^2. When using independent illumination, the illumination power density did not exceed 9.6 mW/mm^2 [13, 14]. Figure 9 demonstrates a variant of a laboratory setup with BA1, BA2 and the developed high-voltage power supply.

5 Conclusion

A two-channel high-voltage pulsed power supply for metal vapor lasers with a repetition rate of 16-24 kHz and a maximum power of 1.2 kW, total over two channels, has been developed. A common inverter circuit provides a synchronous pulsed charge of two storage capacitances, which can differ significantly. In this case, the charge can be carried out through the by-pass inductance (traditional GDT) or through the plasma resistance (capacitive GDT). The voltages on the storage capacitances are equalized by a two-winding inductor located in series in the charge circuit. This approach ensures the spread of the voltage value on the storage capacitor at the moment of turning on the thyratron by no more than 2% at a voltage amplitude of up to 6.5 kV. The wall-plug efficiency of the inverter module is 90-92%, taking into account the power consumed by the thyratron module.

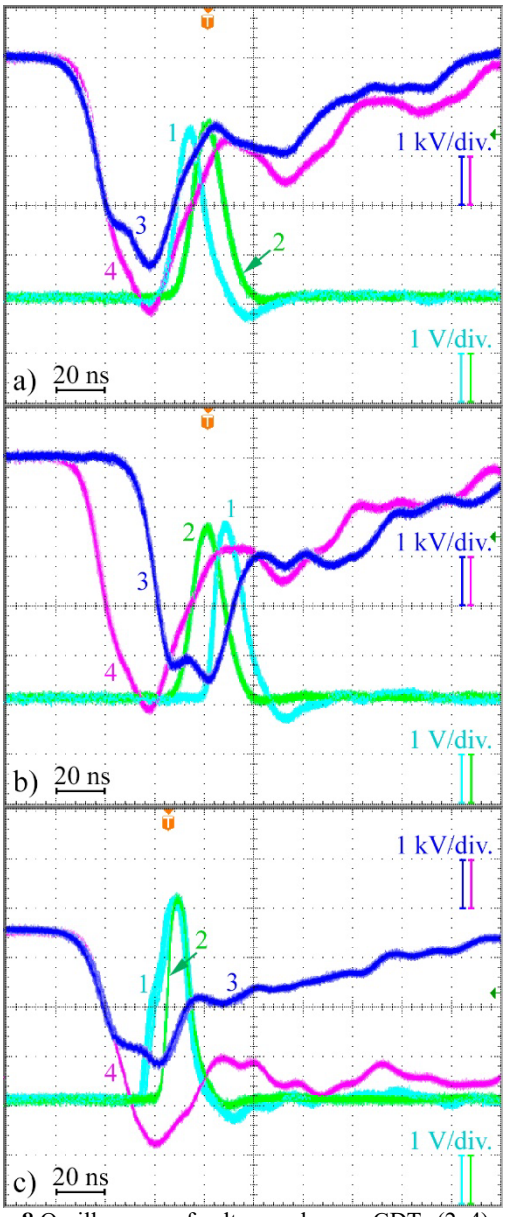

Fig. 8 Oscillograms of voltage pulses on GDTs (2, 4) and lasing (1, 3). (a), (b) – BA1 (2, 4) and BA2 (1, 2) with different delays; (c) – BA2 (1, 2) and BA3 (2, 4), different types of electrodes.

The converter regulation is digitally implemented using a signal processor. The use of the slave control principle, where the input inductor current of the inverter serves as an internal variable, and the input capacitor voltage of the inverter serves as an external variable, ensured high charge stability of the storage capacitors. The use of a single-channel transistor modulator and ferrovariometer-based adjustable delay lines ensured a high stability of the pumping pulses and an accuracy of lasing pulses synchronization of up to ±1 ns. The power supply system includes two separate modules operating with forced air-cooling, which is convenient for its use in portable laser monitoring systems. As a further work, the dimensions of the thyratron module can be reduced by using non-heated cathode thyratrons, which have smaller dimensions and do not require filament transformers. The results obtained can be successfully applied in the creation of high-power systems of synchronized generation based on pulsed metal vapor lasers and used in various fields of pulsed technology.

Intellectual Property

The authors confirm that they have given due consideration to the protection of intellectual property associated with this work and that there are no impediments to publication, including the timing to publication, with respect to intellectual property.

Funding

No funding was received for this work

Credit Authorship Contribution Statement

E. Y. Burkin: Research & Investigation, Idea & Conceptualization, Software and Simulation, Original Draft Preparation, Data Curation, Verification. **F. A. Gubarev:** Supervision, Idea & Conceptualization, Methodology, Analysis, Research & Investigation, Data Curation, Original Draft Preparation, Revise & Editing. **V. V. Sviridov:** Research & Investigation, Data Curation, Original Draft Preparation. **D. V. Shiyanov:** Methodology, Research & Investigation.

Declaration of Competing Interest

The authors hereby confirm that the submitted manuscript is an original work and has not been published so far, is not under consideration for publication by any other journal and will not be submitted to any other journal until the decision will be made by this journal. All authors have approved the manuscript and agree with its submission to "Iranian Journal of Electrical and Electronic Engineering".

References

[1] G. S. Evtushenko, Methods and instruments for visual and optical diagnostics of objects and fast processes. New York, USA: Nova Science Publishers, 2018.

[2] G. S. Evtushenko, M. V. Trigub, F. A. Gubarev, T. G. Evtushenko, S. N. Torgaev, and D. V. Shiyanov, "Laser monitor for non-destructive testing of materials and processes shielded by intensive background lighting," *Review of Scientific Instruments*, Vol. 85, No.3, p. 033111, 2014.

[3] R. O. Buzhinsky, V. V. Savransky, K. I. Zemskov, A. A. Isaev, and O. I. Buzhinsky, "Observation of objects under intense plasma background illumination," *Plasma Physics Reports*, Vol. 36, No. 13, pp. 1269-1271, 2010.

[4] D. V. Abramov, S. M. Arakelian, A. F. Galkin, I. I. Klimovskii, A. O. Kucherik, and V. G. Prokoshev, "On the possibility of studying the temporal evolution of a surface relief directly during exposure to high-power radiation", *Quantum Electronics*, Vol. 36, No. 6, pp. 569-575, 2006.

[5] A. P. Kuznetsov, R. O. Buzhinskij, K. L. Gubskii, A. S. Savjolov, S. A. Sarantsev, and A. N. Terekhin, "Visualization of plasma-induced processes by a projection system with a Cu-laser-based brightness amplifier", *Plasma Physics Reports*, Vol. 36, No. 5, pp. 428-437, 2010.

[6] O. I. Buzhinskij, V. G. Otroshchenko, A. A. Slivitsky and I. A. Slivitskaya, "Videoscope on the basis of copper vapor laser for spatially-temporal diagnostics of tokamak discharge chamber internal components," *Plasma Devices and Operations*, Vol. 11, No. 3, pp. 155-160, 2003.

[7] D. V. Beloplotov, M. V. Trigub, V. F. Tarasenko, G. S. Evtushenko, and M. I. Lomaev, "Laser monitor visualization of gas-

dynamic processes under pulse-periodic discharges initiated by runaway electrons in atmospheric pressure air," *Atmospheric and Oceanic Optics*, Vol. 29, No. 4, pp. 371-375, 2016.

[8] L. Li, A. V. Mostovshchikov, A. P. Ilyin, D. V. Shiyanov, and F. A. Gubarev, "In situ nanopowder combustion visualization using laser systems with brightness amplification," *Proceedings of the Combustion Institute*, Vol. 38, No. 1, pp. 1695-1702, 2021.

[9] L. Li, D. V. Shiyanov and F. A. Gubarev, "Spatial-temporal radiation distribution in a CuBr vapor brightness amplifier in a real laser monitor scheme," *Applied Physics B*, Vol. 126, No 10, 2020.

[10] A. G. Grigor'yants, M. A. Kazaryan and N. A. Lyabin, *Laser precision microprocessing of materials*. Boca Raton, USA: CRC Press, 2019.

[11] D. W. Coutts, "Double-pass copper vapor laser master-oscillator power-amplifier systems: generation of flat-top focused beams for fiber coupling and percussion drilling," *IEEE Journal of Quantum Electronics*, Vol. 38, No. 9, pp. 1217-1224, 2002.

[12] M. V. Trigub, N. A. Vasnev, and G. S. Evtushenko, "Bistatic laser monitor for imaging objects and processes," *Applied Physics B*, Vol. 126, No. 3, pp. 1-7, 2020.

[13] A. Y. Dolgoborodov, V. G. Kirilenko, M. A. Brazhnikov, L. I. Grishin, M. L. Kuskov, and G. E. Valyano, "Ignition of nanothermites by a laser diode pulse," *Defence Technology*, Vol. 18, No. 2, pp. 194-204, 2022.

[14] F. A. Gubarev, E. Y. Burkin, A. V. Mostovshchikov, A. P. Ilyin, and L. Li, "Two-channel system with brightness amplification for monitoring the combustion of aluminum-based nanopowders," *IEEE Transactions on Instrumentation and Measurement*, Vol. 70, pp. 1-9, 2021.

[15] A. S. Moldabekov, F. A. Gubarev, and A. V. Mostovshchikov, "Laser monitor with independent illumination from capacitive-discharge-pumped CuBr laser for metal nanopowder combustion study," *International Conference of Young Specialists on Micro/Nanotechnologies and Electron Devices, EDM*, pp. 273-278, 2021.

[16] C. E. Little, *Metal Vapor Lasers: Physics, Engineering and Applications*. *Chichester, ENG: John Wiley & Sons Ltd*., 1999.

[17] V. M. Batenin, P. A. Bokhan, V. V. Buchanov, G. S. Evtushenko, M. I. Kazaryan, V. T. Karpukhin, I. I. Klimovskii, and M. M. Malikov, *Lasers on self-terminating transitions in metal vapors – 2*. Moscow: RUS: Fizmatlit, 2011.

[18] D. V. Shiyanov, G. S. Evtushenko, V. B. Sukhanov, and V. F. Fedorov, "A copper bromide vapour laser with a high pulse repetition rate," *Quantum Electronics*, Vol. 32, No. 8, pp. 680-682, 2002.

[19] G. N. Tiwari, P. K. Shukla, R. K. Mishra,V. K. Shrivastava, R. Khare, and S. V. Nakhe, "Effect of addition of hydrogen to neon buffer gas of copper bromide vapour laser on its spectral and temporal characteristics," *Optics Communications*, Vol. 338, pp. 322-327, 2015.

[20] I. K. Kostadinov, K. A. Temelkov, D. N. Astadjov, S. I. Slaveeva, G. P. Yankov, and N. V. Sabotinov, "High-power copper bromide vapor laser," *Optics Communications*, Vol. 501, p.127363, 2021.

[21] V. A. Dimaki, V. B. Sukhanov, V. O. Troitskii, and A. G. Filonov, "A stabilized copper bromide laser with computer-controlled operating modes and a mean lasing power of 20 W" , *Instruments and Experimental Techniques*, Vol. 55, pp. 696-700, 2012.

[22] F. A. Gubarev, M. V. Trigub, G. S. Evtushenko, and K. V. Fedorov, "Influence of the discharge circuit inductance on output characteristics of a CuBr laser," *Atmospheric and Oceanic Optics*, Vol. 26, No. 6, pp. 559-564, 2013.

[23] M. V. Trigub, V.O. Troitskii, and V. A. Dimaki, "Continuous control of CuBr laser pulse energy," *Optics & Laser Technology*, Vol. 139, p.106929, 2021.

[24] F. A. Gubarev, D. V. Shiyanov, V. B. Sukhanov, and G. S. Evtushenko, "Capacitive-discharge-pumped CuBr laser

with 12 W average output power," *IEEE Journal of Quantum Electronics*, Vol. 49, No. 1, pp. 89-94, 2013.

[25] D. V. Shiyanov, V. B. Sukhanov, and F. A. Gubarev, "Influence of peaking capacitance on the output power of capacitive-discharge-pumped metal halide vapor lasers," *IEEE Journal of Quantum Electronics*, Vol. 54, No. 2, p. 1500107, 2018.

[26] S. V. Nakhe, B. S. Rajanikanth, and R. Bhatnagar, "Energy deposition studies in a copper vapor laser under different pulse excitation schemes" *Measurement Science and Technology*. , Vol. 14, pp. 607-613, 2003.

[27] B. S. Tsikimis, T. Ch. Chardalias, A. K. Ftoulis, J. M. Koutsoubis, and Ch. X. Manasis, "A fast, high-voltage, pulse power driving circuit for copper-halide lasers", *ICHVE 2018 - 2018 IEEE International Conference on High Voltage Engineering and Application*, p. 8641760, 2019.

[28] A. J. Andrews, R. C. Tobin and C. E. Webb, "Driving circuits for copper halide lasers – a parametric study", *Journal of Physics D: Applied* Physics, Vol. 13, pp. 1017-1027, 1980.

[29] LLC "Pulsed Technologies", *Pulse thyratrons – high-current pseudo-spark switches of the TPI series*. URL: https://www.pulsetech.ru/pages/produkciya/impulsnye-tiratrony-silnotochnye-psevdoiskrovye-kommutatory-serii-tpi.

E. Y. Burkin was born in Stepnogorsk town, Kazakhstan Republic, USSR on December 28, 1971. He graduated from Tomsk Polytechnic University (TPU) in 1994, has diploma of Master of techniques and technology on the direction "Electronics and Microelectronics". In 1998, he received PhD in Power Electronics. During 1998-2013, he was a lecturer, during 2013-2020 – an associated professor of TPU. He is a leading engineer of the laboratory of pulse-beam, electric discharge and plasma technologies in TPU. His area of scientific activity is high voltage power supplies and their applications.

F. A. Gubarev was born in Leninogorsk town (now Ridder), Kazakhstan Republic, USSR on November 15, 1979. He graduated from Tomsk Polytechnic University (TPU) in 2003, has diploma of Master of techniques and technology on the direction "Electronics and Microelectronics". In 2008, he received PhD in Physics. In 2022, he received ScD in Physics. Since 2003, he has been involved in the investigation and design of metal compound vapor lasers and brightness amplifiers. His area of scientific activity is photonics, lasers and their applications. Now he is a professor of Sevastopol State University.

V. V. Sviridov was born in Karagandinsky village, Kazakhstan Republic, USSR on June 23, 1965. He graduated from Tomsk Polytechnic Institute (TPI) in 1992, has diploma of Master of techniques and technology on the direction "Electronics and Microelectronics". He is a leading engineer of the laboratory of pulse-beam, electric discharge and plasma technologies in TPU. His area of scientific activity is industrial electronics, high voltage power supplies and their applications.

D. V. Shiyanov was born in Tomsk city, USSR in 1973. He graduated from Tomsk State University (radio-physical faculty) in 1998. In 2007, he has received PhD in Physics. Since 1999, D. Shiyanov has been involved in the investigation and design of metal compound vapor lasers. He has published over 70 papers in this area including two monographs. Now he is a senior researcher officer of Quantum Electronics Laboratory of V.E. Zuev Institute of Atmospheric Optics, Siberian Branch of Russian Academy of Science.